Modification of the physicochemical properties of commercial TiO$_2$ samples by soft mechanical activation

M.C. Hidalgo [b,*], G. Colón [a], J.A. Navío [a]

[a] *Instituto de Ciencia de Materiales de Sevilla (ICMSE), Centro mixto CSIC-Universidad de Sevilla,*
Avda. Americo Vespucio, s/n 41092 Sevilla, Spain
[b] *Institute für Solarenergieforschung Hameln/Emmerthal (ISFH), Aussenstelle Hannover Sokelantstrasse 5, D-30165 Hannover, Germany*

Abstract

The modifications of the physicochemical properties, such as the crystalline phase composition, of two commercial TiO$_2$ samples (Degussa P25 and Hombikat UV-100) by soft mechanical treatment have been studied.

Original and modified TiO$_2$ samples were widely characterized (XRD, BET surface area and pore size distribution, SEM/TEM, XPS and DR/UV–Vis). Certain structural and morphological differences were found after the mechanical treatment of the oxides, which depended on the initial phase composition of the oxide, and thus, on the kind of TiO$_2$ sample. The photoactivities exhibited by original commercial (non-modified) TiO$_2$ and the modified ones were tested for Cr(VI) photoreduction.

Changes generated by soft mechanical treatment lead to a considerably modification in the intrinsic physicochemical properties of the non-modified TiO$_2$ samples, inducing a decrease in their photoactivities. This loss of photoactivity could be a problem from the point of view of reutilization of the photocatalyst powder in big real collectors, where the photocatalyst particles are subjected to continuous collisions close to the soft mechanical activation conditions reported here. This is specially important for the TiO$_2$ Degussa P25 sample, which after a short time of soft mechanical treatment shows a high alteration of its physicochemical properties and thus, in its photocatalytic activity. © 2002 Elsevier Science B.V. All rights reserved.

Keywords: TiO$_2$; Grinding; Polymorphic transformation; Photocatalysis; Cr(VI); Photoreduction

1. Introduction

Mechanical treatment applied to a material, besides modifying its granulometric distribution, can have a marked influence in its physical properties and its chemical reactivity; particularly, the nature and phase composition, as well as the texture and morphology of particles can be noticeable modified [1–8]. The influence of mechanical activation in the polymorphic transformation kinetics is due to a change in the geometric boundary conditions and the introduction of an excess of energy in the solid structure during the grinding treatment. This change in the energy state of the solid can lead to the formation of metastable phases at room temperature and pressure, otherwise existing at equilibrium only at high temperatures and/or high pressures.

The grinding of materials is a complex process, which depends on many factors, such as the kind of mill used, nature and properties of the balls and cups, and milling conditions (temperature, atmosphere, amount and chemical composition of the grinding material, etc.) [1–8].

TiO$_2$ presents three natural polymorphic phases: anatase, rutile and brookite. Other high-pressure forms are also known, α-PbO$_2$ type and baddeleyite type. Mechanically activated transition of anatase to rutile phase in TiO$_2$ at room temperature by ball-milling has been object of interest in numerous studies [2–5,8]. Anatase is being considered as the most photoactive phase of this oxide; however, commercial TiO$_2$ Degussa P25, with a phase ratio anatase to rutile 80:20, has shown a high photoactivity for most of the processes studied [9]. In any way, it is commonly accepted that the phase composition of a TiO$_2$ sample is the paramount importance for its photocatalytic activity [10–13].

In this paper we have studied the modifications of the physicochemical properties, such as the crystalline phase composition, of two of the most widely known commercial TiO$_2$ samples (Degussa P25 and Hombikat UV-100) by low-energy mechanical treatment, and the influence that these modifications have in their photocatalytic activities, tested in the photoreduction of Cr(VI).

* Corresponding author. Tel.: +49-511-35850144;
fax: +49-511-35850110.
E-mail address: chidalgo@cica.es (M.C. Hidalgo).

2. Experimental

2.1. Materials and methods

Degussa P25 and Hombikat UV-100 (Sachtleben Chemie) commercial titanium dioxide were used in the grinding studies as received. A mixing-mill (Retsch model MM2000) was used for transversal-agitation of two agate cups of ca. 10 ml at an oscillation frequency of 13 Hz, containing a ball of the same material in each cup (7 mm in diameter). For the treatment of TiO_2 Degussa P25 sample, 0.30 g of this powder was settled in each cup and agitated for 0.5–25 h. For TiO_2 Hombikat UV-100 sample 1.0 g was agitated in each cup for 0.5–180 h. In both cases the samples occupied a third part of the cup volume.

Photocatalytic runs were performed in a Pyrex immersion well reactor. UV illumination of the reaction solutions was provided by a medium pressure 400 W Hg lamp supplied by Applied Photophysics. Actinometric measurements were carried out by using the chemical actinometer Aberchrome 540 [14]. A photon flow of 2.6×10^{-7} Einstein dm^{-3} s^{-1} was calculated.

Cr(VI) solutions were prepared from analytical grade $K_2Cr_2O_7$ Aldrich 99%, using H_2SO_4 to adjusting the pH to 2. In all cases, 1 g/l of the catalyst was suspended in 4×10^{-4} M solutions and oxygen flow was employed to produce a homogeneous suspension. Prior to illumination, the suspensions were stirred in the dark for 20 min, sufficient time to reach the catalyst–substrate equilibrium. Cr(VI) concentrations were measured by UV–Vis spectroscopy, using its characteristic 290 nm band. Samples of about 2 ml were removed periodically during the experiments and filtered (millipore Milex25 0.45 μm membrane filter) prior to UV–Vis spectra measurements.

2.2. Characterization

X-ray diffraction (XRD) patterns were obtained with a Siemens D-501 diffractometer using Cu Kα radiation and equipped with a Ni filter and a graphite monochromator. The identification of the different crystalline phases in the spectra was accomplished using the JCPDS database.

Transmission electron microscopy (TEM) was performed using a Philips CM 200 electronic microscope. The microscope was equipped with a top-entry holder and ion pumping system, operating at an accelerating voltage of 200 kV and giving a nominal structural resolution of 0.21 nm. Samples were prepared by dipping a 3 mm holed carbon grid into ultrasonic dispersion of the oxide powder in ethanol.

Scanning electron microscopy (SEM) was performed on gold-coated samples using a Jeol apparatus model JSM-5400, equipped with a Link analyzer, model ISIS, for X-ray energy-dispersive analyses (EDX).

BET surface area measurements and pore size distributions were carried out by N_2 adsorption at 77 K using a Micromeritics ASAP 2010 analyzer. Pore volumes were

determined by applying the Barret–Joyner–Halenda (BJH) method to the desorption branch of the N_2 isotherms.

UV–Vis spectra were measured on a Shimadzu UV-2101 apparatus, equipped with an integrating sphere, and using Ba_2SO_4 as reference. The spectra were recorded in diffuse reflectance mode and transformed to a magnitude proportional to the extinction coefficient (κ) thought the Kubelka–Munk function ($F(R_\infty)$).

X-ray photoelectron spectroscopy (XPS) was carried out on a Leybold Heraeus LHS-10 spectrometer, working with constant pass energy of 50 eV, and using Al Kα radiation as excitation source. Before XPS recording a final pressure of 10^{-9} Torr was attained. C(1s) signal was used as internal reference.

3. Results and discussions

3.1. Structure and morphology characterization

The XRD profiles of the TiO_2 Degussa P25 and Hombikat UV-100 samples ground for different times are shown in Figs. 1 and 2, respectively. Non-modified TiO_2 Degussa P25 sample shows a phase composition of 80:20 anatase to rutile.
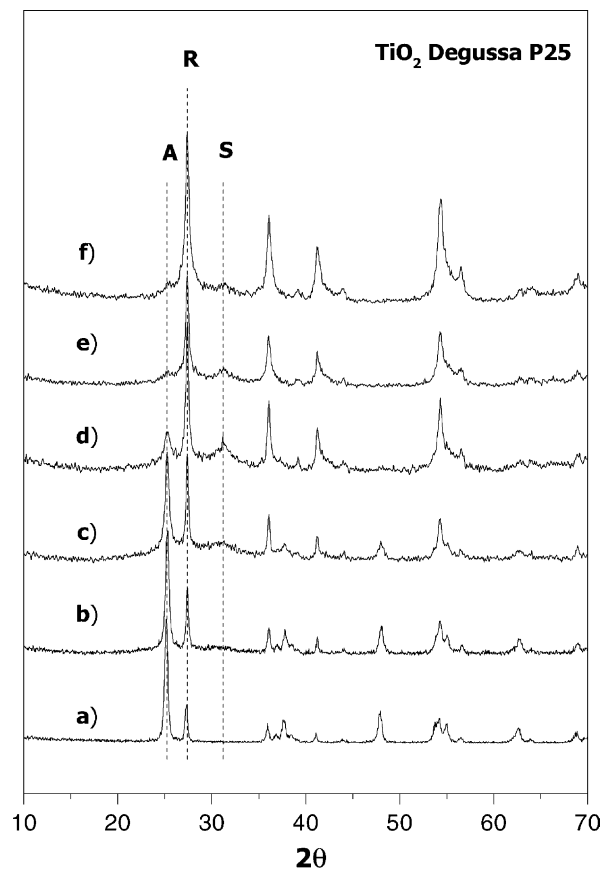

Fig. 1. X-ray patterns, showing lines characteristic of anatase (A), rutile (R) and TiO_2-II α-PbO$_2$-type structure (S), of TiO_2 Degussa P25 (a) non-modified, and agitated in the mixing-mill for: (b) 1 h; (c) 3 h; (d) 8 h; (e) 12 h; and (f) 20 h.
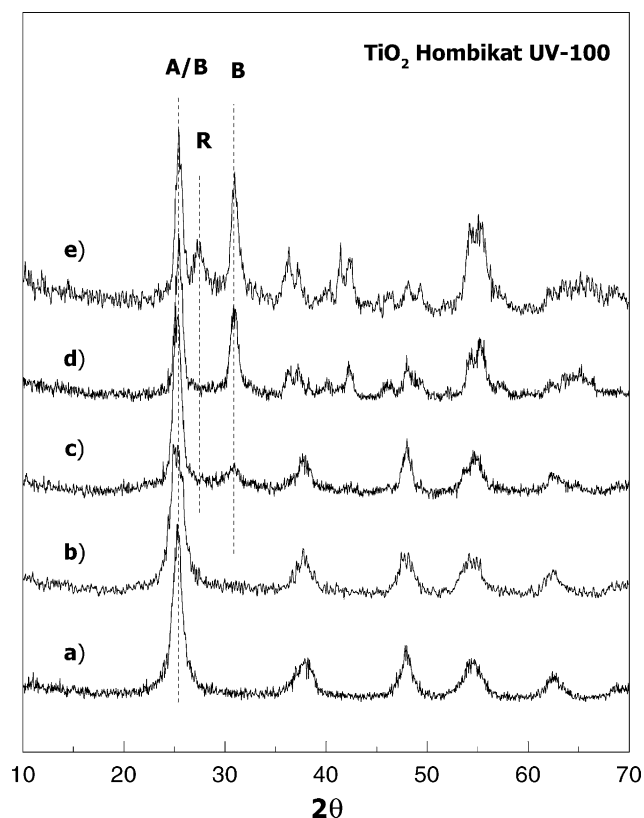
Fig. 2. X-ray patterns, showing lines characteristic of anatase (A), rutile (R) and brookite (B), of TiO$_2$ Hombikat UV-100 (a) non-modified, and agitated in the mixing-mill for: (b) 10 h; (c) 50 h; (d) 100 h; and (e) 180 h.

As it can be observed in Fig. 1, the fraction of anatase phase in this sample was decreasing rapidly with increasing milling times, and transformed to rutile through a transient phase, TiO$_2$-II α-PbO$_2$-type structure, that appear after 3 h of treatment, vanishing after prolonged milling times. After milling times longer than 12 h, rutile was the only remaining phase.

The crystallite sizes for anatase and rutile phases were calculated by means of the Debye–Scherrer equation [15] using the main diffraction line for each phase (1 0 1) for anatase and (1 1 0) for rutile. For both phases, a decrease in the crystallite size was produced with the mechanical treatment. Anatase crystals for the non-modified sample were around 20 nm, and were decreasing linearly with grinding time until this phase was completely disappeared, being about 7 nm after 8 h. Rutile crystals were decreasing too, from around 33 nm of the non-modified sample to about 17 nm after 25 h of treatment.

Non-modified TiO$_2$ Hombikat UV-100 presents anatase as only crystalline phase. With mechanical treatment, the anatase phase was transformed into brookite (Fig. 2), and after 150 h of milling, this is the only phase observed. For longer times, rutile phase was formed, co-existing with brookite.

Due to the overlapping of the main diffraction peaks of anatase (1 0 1) and brookite (1 2 0), the crystallite size for anatase could not be calculated for this sample as a function

of milling time. Instead, the second peak in intensity for brookite phase (1 2 1) was used to estimate the crystallite size of this phase. A linear increment with grinding time was observed, the crystallite sizes for brookite phase after 50 h of grinding were about 5 nm and they were increasing until around 10 nm after 150 h.

One first important difference can be found here between the two samples studied. In TiO$_2$ Degussa P25 sample, the anatase phase rapidly disappeared, and after only 30 min of treatment, the phase composition of this sample have been altered notably. By contrast, for TiO$_2$ Hombikat UV-100 sample, changes in phase composition are produced slowly, and 50 h of milling are necessary to observe a decreasing of the anatase phase.

The morphology of the particles was observed under TEM, and the pictures of selected samples are shown in Fig. 3. For TiO$_2$ Degussa P25 sample (Fig. 3(a) and (b)) a certain increase of the amorphous degree could be observed with milling time and the tendency of the primary particles to agglomerate at prolonged milling times.

As Fig. 3(c) and (d) shows, an increase of primary particle size in TiO$_2$ Hombikat UV-100 sample as a function of grinding took place. This tendency was maintained for treatments longer than 50 h, and TEM images of these samples shows an increasing in the primary particle sizes with increasing milling times (pictures not shown). These results are in agreement with the increasing values of crystallite size calculated for this sample as a function of grinding time by the Debye–Scherrer equation. This could be explained by assuming that the lattice defects generated during the milling promoted cold-welding of the new brookite particles. The observation of these TEM micrographs also suggests that

Table 1
Specific surface area, S_{BET}, for TiO$_2$ Degussa P25 and Hombikat UV-100 after the indicated milling times

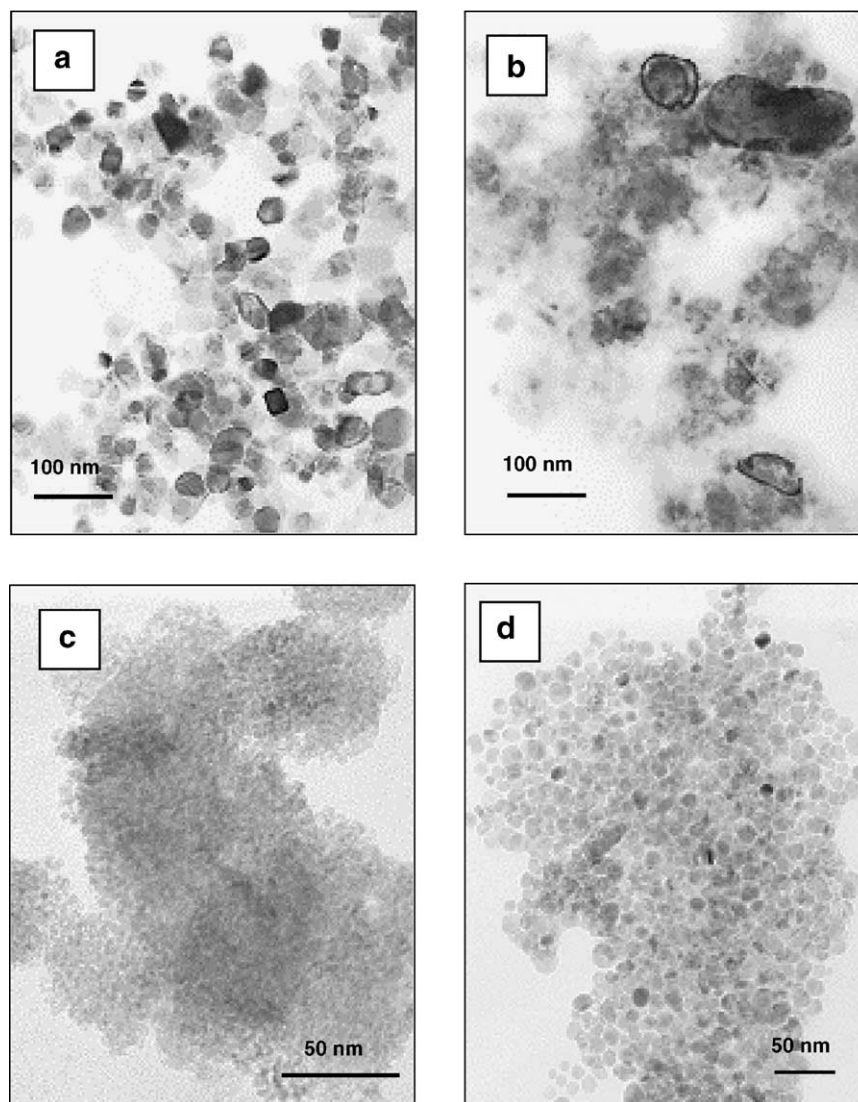|	S_{BET} (m^2/g)
Degussa P25 Milling time (h)	
0	50
0.5	52
1	54
3	55
5	54
8	63
10	66
12	70
15	61
20	58
25	56
Hombikat UV-100 Milling time (h)	
0	290
10	164
20	160
50	135
75	133
100	100
150	96
180	83

Fig. 3. Transmission electron micrographs of TiO_2 Degussa P25 (a) non-modified; (b) after 10 h of milling, and TiO_2 Hombikat UV-100; (c) non-modified; and (d) after 50 h of milling.

there is not an increase of amorphous character during the milling process in this sample.

Specific surface area, S_{BET}, values for both TiO_2 samples after milling are shown in Table 1. For Degussa P25 sample, S_{BET} increased with grinding time, from $50\,m^2/g$ of the non-modified sample to $70\,m^2/g$ after 12 h of milling, and then decreased slightly for longer agitation times. This increment in surface area for shorter grinding time could be ascribed to the breaking of larger crystals. The decreasing in anatase crystal sizes (confirmed in XRD studies), together with the lattice distortion and the excess of energy produced by the mechanical treatment, can be the causes for the rapidly transformation of anatase into rutile phase in this sample. The different densities between these two phases ($\varphi_A = 3.88\,g/cm^3$, $\varphi_R = 4.26\,g/cm^3$) and the agglomeration of secondary particles with plugging of pores, could

cause the decreasing in the specific surface area observed for greater milling times.

In the TiO_2 Hombikat UV-100 sample (Table 1), the specific surface area decreased notably with the mechanical treatment, from $290\,m^2/g$ of the non-modified sample to $164\,m^2/g$ after 10 h of grinding, and $83\,m^2/g$ after 180 h. The decrease in S_{BET} can be attributed to the plugging of micropores as a result of the agglomeration and densification of the secondary particles, producing a loosing of pores between primary particles. This effect was confirmed by SEM, where the tendency of the particles to agglomerate with grinding time could be observed (results not shown).

Fig. 4 shows the pore size distribution for TiO_2 Degussa P25 and Hombikat UV-100, non-modified samples and after different milling times. The non-modified Degussa P25 sample presents a wide pore distribution in mesopore range
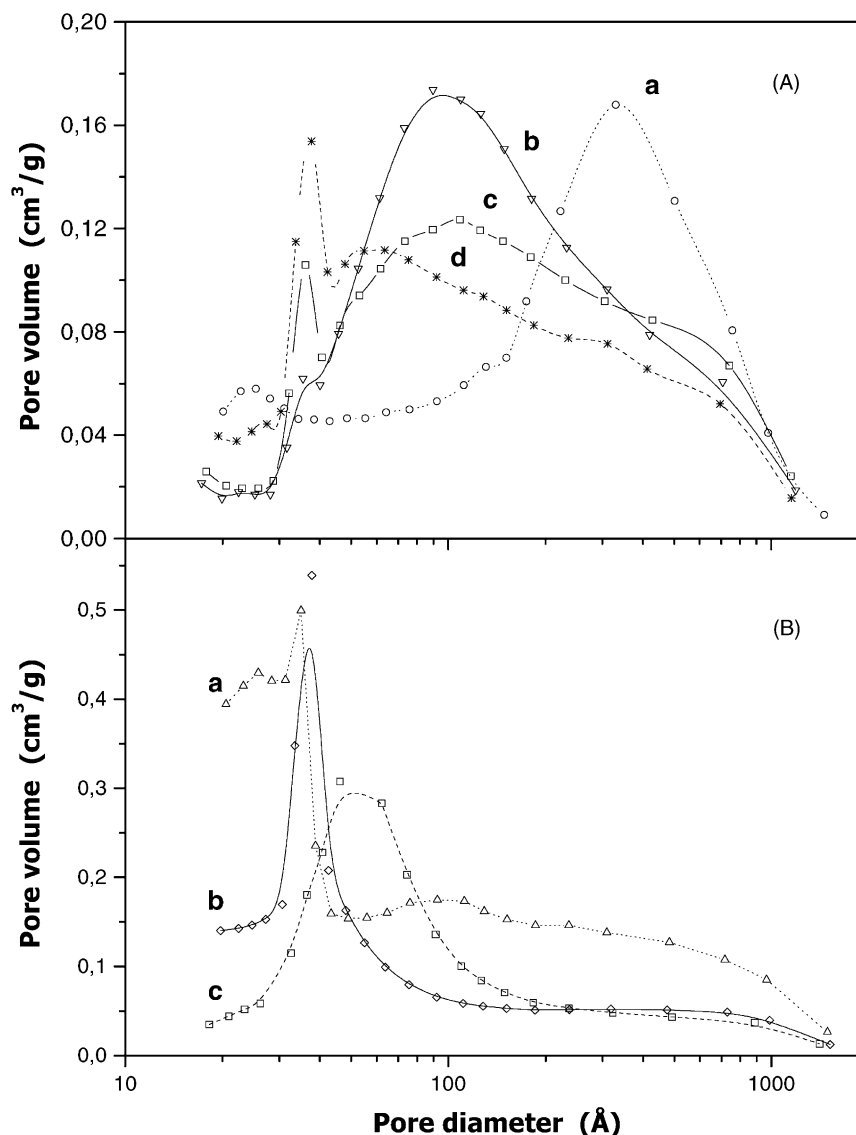
Fig. 4. Pore size distribution for (A) TiO$_2$ Degussa P25 (a) non-modified, and agitated in the mixing-mill for: (b) 1 h; (c) 3 h; (d) 10 h; and (B) TiO$_2$ Hombikat UV-100 (a) non-modified, and agitated in the mixing-mill for: (b) 50 h; (c) 150 h.

(20–500 Å). As one can observe in Fig. 4A, the maximum of pore volume is shifted to lower pore diameters with milling time. This effect would be in agreement with the increasing of surface area observed for this sample, ascribed to the disaggregation and breaking of particles and the subsequent creation of smaller pores. Just the opposite effect can be observed for TiO$_2$ Hombikat UV-100 in Fig. 4B. The non-modified sample presents a wide pore distribution in mesopore range like Degussa P25, but also in micropore range, and the maximum of pore volume suffers a shift to higher pore diameters with the agitation time. This suggests the loss of the smaller pores with milling treatment, which would be in agreement with the decreasing of surface area observed for this sample.

Diffuse reflectance spectroscopy studies (Fig. 5), for non-modified and mechanically treated samples, showed that milling treatment altered slightly the absorption properties in both commercial TiO$_2$ samples. Absorption is produced in the original samples at wavelengths lower than 400 nm. With mechanical treatment the absorption edges were shifted slightly at higher wavelengths, and thus the band gap energies decreased from 3.5 eV of the non-modified samples to 3.3 eV after milling treatment (1 h for Degussa P25 and 10 h for Hombikat UV-100). For longer milling times, the band gap values remained in 3.3 eV for both samples. Milling is known to generate accumulations of defects, and the absorption increment observed could be due to the generation of oxygen vacancies in the structure of TiO$_2$ with the milling treatment. This was confirmed for the change of color observed in the powder from white to grayish and for the XPS analysis, where a decreasing in the superficial O/Ti ratio with milling time was produced (data not shown).
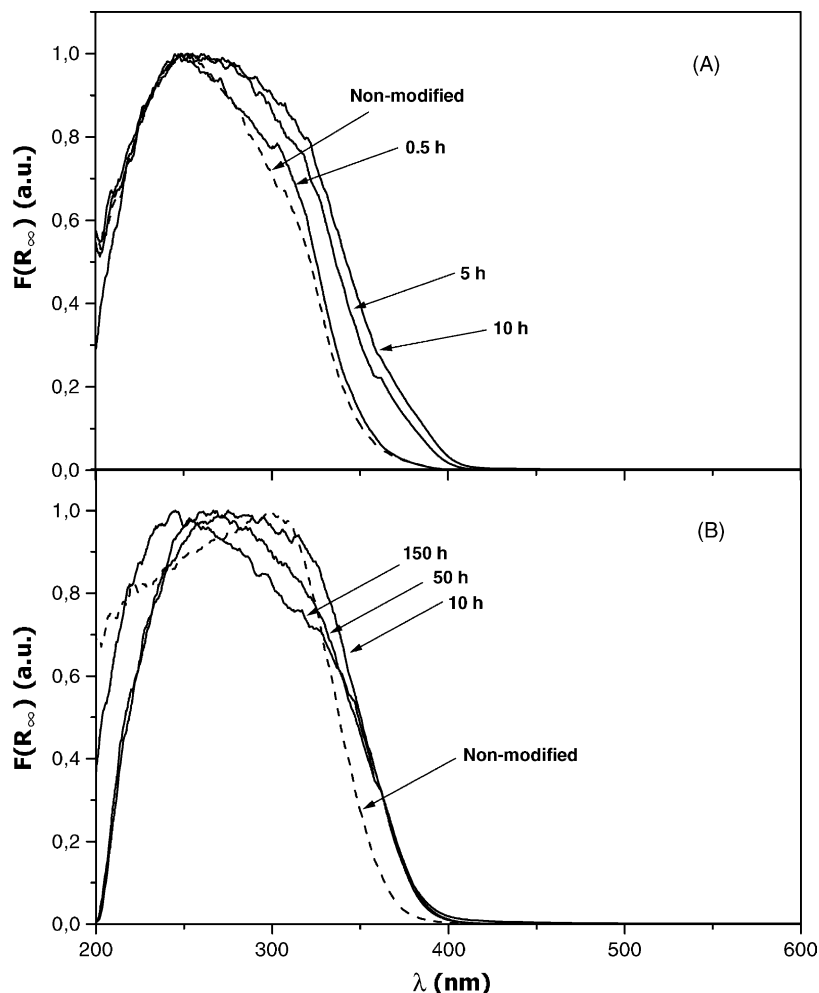
Fig. 5. Diffuse reflectance UV–Vis spectra for TiO$_2$ (A) Degussa P25, and (B) Hombikat UV-100, non-modified samples and after the indicated milling times.

3.2. Photocatalytic properties

TiO$_2$ Degussa P25 and Hombikat UV-100 samples, non-modified and after different milling times, were tested for photoreduction of Cr(VI) in the presence of oxygen flow. The catalyst–substrate suspensions were stirring in the dark for 20 min, time enough to reach the equilibrium powder-Cr(VI) solution, and then irradiated for 8 h.

Fig. 6 shows the time courses of Cr(VI) reduction on TiO$_2$ mechanically modified Degussa P25 and Hombikat UV-100, tested for this reaction. Normalized concentration was plotted against reaction time to avoid slight changes on initial concentration between different experiments. As it can be noticed, the activity of the both photocatalysts decreased notably when the samples were subjected to soft mechanical treatment. The longer was the milling time the higher was the loss of activity. This effect was stronger for TiO$_2$ Degussa P25 sample.

The photonic efficiencies ($\xi\%$) of the different samples for the Cr(VI) reduction were calculated using the following equation [11]:

$$\xi\% = \frac{-\mathrm{d}\,[C]\,/\mathrm{d}t}{P_0} \times 100$$

where $-\mathrm{d}C/\mathrm{d}t$ is the reaction rate and P_0 the incident photonic flow per unit volume (2.6×10^{-7} Einstein dm^{-3} s^{-1}). The photonic efficiency allows only the comparison of experiments performed in similar experimental conditions. The values obtained are shown in Table 2 (initial rates calculated from Fig. 6).

In Table 2, it can be observed that the photonic efficiency for TiO$_2$ Degussa P25 was reduced by more than 50% of its original value only after 1 h of grinding, and it continued decreasing exponentially for longer agitation treatments. The loss of activity can be ascribed to the changes observed in the crystalline phase composition, with the losing of anatase phase, together with the creation of a great amount of defects, which could act as recombination centers for electron–hole pairs. These factors, clearly, did not compensate the higher surface area and the lower bad gap
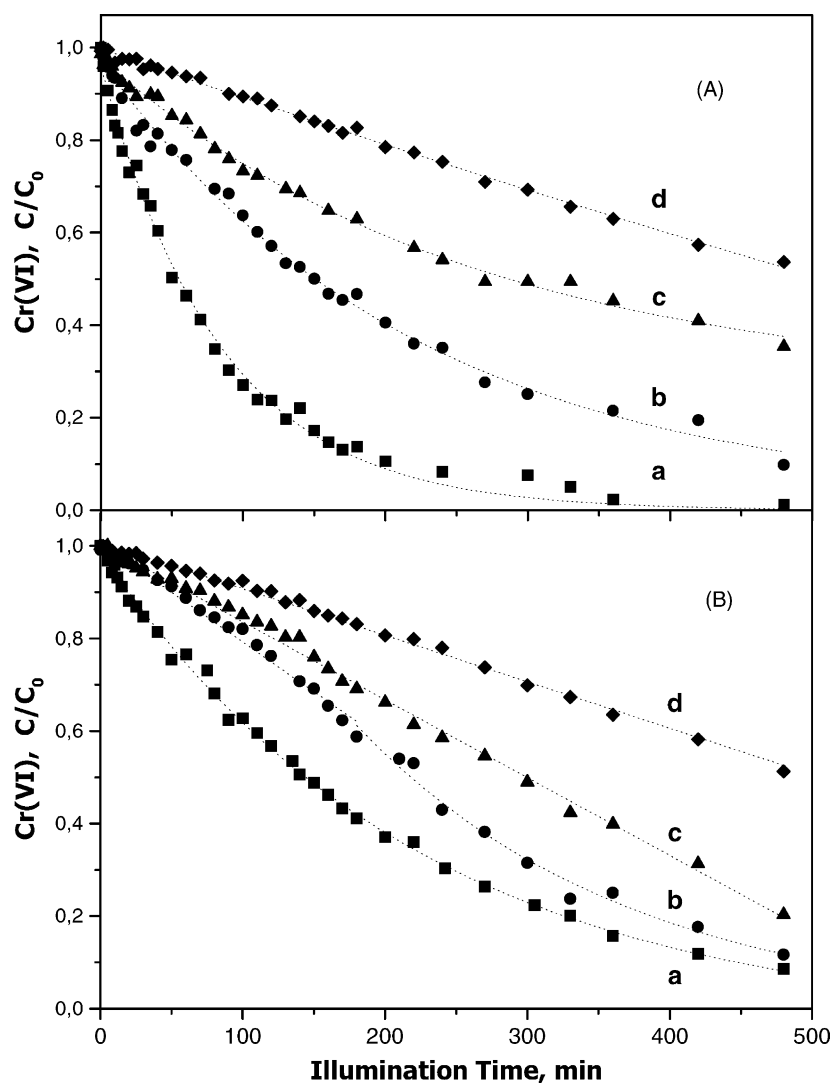
Fig. 6. Normalized concentration vs. illumination time for Cr(VI) reduction over TiO$_2$ (A) Degussa P25, non-modified (a), and after 1 h (b), 10 h (c), and 25 h (d) of milling treatment, and (B) Hombikat UV-100, non-modified (a), and after 10 h (b), 50 h (c), and 150 h (d) of milling treatment. [catalyst] = 1 g/l, [K$_2$Cr$_2$O$_7$]$_0$ = 4 × 10^{-4} mol/l, pH = 2, I_0 = 2.6 × 10^{-7} Einstein dm^{-3} s^{-1}, oxygen bubbling.

Table 2
Calculated photonic efficiencies (ξ%) for the photocatalytic Cr(VI) reduction over TiO$_2$ Degussa P25 and Hombikat UV-100, non-modified and after the indicated milling times

	ξ%
Degussa P25 (h)	
Non-modified	34.6
1	16.0
10	9.9
25	3.0
Hombikat UV-100 (h)	
Non-modified	13.5
10	2.8
50	2.4
150	1.2

energy, a priori positives features for photoactivity, acquired for this sample with grinding treatment.

Photonic efficiencies for TiO$_2$ Hombikat UV-100, collected in Table 2, show also a loss in activity with the mechanical treatment, and after 10 h the photonic efficiency has decreased more than 80%. For longer treatment times, the photonic efficiency decreases slightly with grinding time. Again, the decreasing of activity could be ascribed to the loss of anatase phase with grinding time, in this case transformed into brookite phase, less photoactive. The notably decreasing in surface area and the creation of defects with prolonged milling times could be also factors contributing to the lower activity shown for this sample.

4. Conclusions

The two commercial TiO$_2$ samples studied, Degussa P25 and Hombikat UV-100, show a very different behavior under

low-energy milling conditions, Degussa P25 being the most susceptible to the modification of its physicochemical and surface properties.

Changes generated by low-energy grinding considerably alter the intrinsic physicochemical properties of the non-modified TiO_2 samples, inducing a decrease in their photoactivities. This loss of photoactivity could be a problem from the point of view of reutilization of the photocatalyst powder in large real collectors, where they are subjected to continuous collisions, close to the soft mechanical conditions reported here. The decreasing of activity is specially marked in the TiO_2 Degussa P25 sample, that after a very short time of soft mechanical treatment shows a high alteration of its physicochemical properties and thus, in its photocatalytic activity.

Acknowledgements

References

[1] I.J. Lin, S. Naviv, D.J.M. Grodzian, Miner. Sci. Eng. 7 (1975) 313.
[2] S. Bégin-Colin, T. Girot, G. Le Caër, A. Mocellin, J. Solid State Chem. 149 (2000) 41.
[3] S. Bégin-Colin, T. Girot, A. Mocellin, G. Le Caër, Nanostruct. Mater. 12 (1999) 195.
[4] S. Bégin-Colin, G. Le Caër, A. Mocellin, M. Zandona, E. Bouzy, B. Malaman, J. Alloys Compd. 227 (1995) 157.
[5] J.M. Criado, C. Real, J. Soria, Solid State Ionics 32/33 (1989) 461.
[6] D. Michel, F. Faudot, E. Gaffet, L. Mazerolles, Rev. Metall. 9 (1993) 219.
[7] E.M. Kostic, S.J. Kiss, S.B. Boskovic, S.P. Zec, Am. Ceram. Soc. Bull. 76 (1997) 60.
[8] C. Real, J.M. Criado, V. Balek, J. Mater. Sci. 33 (1998) 5247.
[9] R.I. Bickley, T. González-Carreño, J.S. Leeds, L. Palmisano, R.J.D. Tilley, J. Solid State Chem. 92 (1991) 178.
[10] A.L. Linsebigler, G. Lu, J.T. Yates Jr., Chem. Rev. 95 (1995) 735.
[11] M.R. Hoffmann, S.T. Martin, W. Choi, D.W. Bahnemann, Chem. Rev. 95 (1995) 69.
[12] S.J. Tsai, S. Cheng, Catal. Today 33 (1997) 227.
[13] A.P. Rivera, K. Tanaka, T. Hisanaga, Appl. Catal. B 3 (1993) 37.
[14] H.G. Heller, J.R. Langan, J. Chem. Soc., Perkin Trans. II (1981) 341.
[15] B.D. Cullity, in: Elements of X-ray Diffraction, Addison-Wesley, Reading, MA, 1956.